Original Article

Quantitative peripheral live single T-cell dynamic polyfunctionality profiling predicts lung cancer checkpoint immunotherapy treatment response and clinical outcomes

Zuan-Fu Lim[1,2], Xiaoliang Wu[2], Lin Zhu[2], Heidar Albandar[3], Maria Hafez[3], Chenchen Zhao[2], Mohammed Almubarak[3,4], Matthew Smolkin[5], Hong Zheng[2], Sijin Wen[6], Patrick C. Ma[2]

[1]Cancer Cell Biology Program, West Virginia University School of Medicine, West Virginia University, Morgantown, WV, USA; [2]Penn State Cancer Institute, Penn State Health Milton S. Hershey Medical Center, Penn State College of Medicine, Penn State University, Hershey, PA, USA; [3]WVU Cancer Institute, Mary Babb Randolph Cancer Center, West Virginia University School of Medicine, West Virginia University, Morgantown, WV, USA; [4]Division of Hematology & Oncology, Mary Babb Randolph Cancer Center, West Virginia University, Morgantown, WV, USA; [5]Department of Pathology, West Virginia University School of Medicine, Morgantown, WV, USA; [6]Department of Biostatistics, School of Public Health, West Virginia University, Morgantown, WV, USA

Contributions: (I) Conception and design: ZF Lim, X Wu, PC Ma; (II) Administrative support: H Albandar, M Hafez, PC Ma; (III) Provision of study materials or patients: C Zhao, M Almubarak, M Smolkin, H Zheng, PC Ma; (IV) Collection and assembly of data: ZF Lim, X Wu, L Zhu, PC Ma; (V) Data analysis and interpretation: ZF Lim, S Wen, PC Ma; (VI) Manuscript writing: All authors; (VII) Final approval of manuscript: All authors.

Correspondence to: Patrick C. Ma, MD, MSc. Professor of Medicine and Microbiology & Immunology, Interim Chief, Division of Hematology/Oncology, Associate Director of Translational Research, Penn State Cancer Institute, Penn State Health Milton S. Hershey Medical Center, Penn State College of Medicine, Penn State University, 400 University Drive, P.O. Box 850, Mail Code CH46, Hershey, PA 17033, USA. Email: patrickma@pennstatehealth.psu.edu.

Background: Predictive biomarkers for immune checkpoint inhibitors (ICIs), e.g., programmed death ligand-1 (PD-L1) tumor proportional score (TPS), remain limited in clinical applications. Predictive biomarkers that require invasive tumor biopsy procedures are practically challenging especially when longitudinal follow-up is required. Clinical utility of tissue-based PD-L1 TPS also becomes diluted when ICI is combined with chemotherapies. Peripheral single T-cell dynamic polyfunctionality profiling offers the opportunity to reveal rare T-cell subpopulations that are polyfunctional and responsible for the underlying ICI treatment molecular response that bulk biological assays cannot achieve. Here, we evaluated a novel live single-cell functional liquid biopsy cytokine profiling platform, IsoLight, as a potential predictive biomarker to track ICI treatment response and clinical outcomes in non-small cell lung cancer (NSCLC).

Methods: Peripheral blood mononuclear cell samples of 10 healthy donors and 10 NSCLC patients undergoing ICI-based therapies were collected longitudinally pre-/post-ICI treatment after ≥2 cycles under institutional review board (IRB)-approved protocols. Cancer blood samples were collected from unresectable advanced stage (III–IV) NSCLC patients. Clinical course and treatment response and survival outcomes were extracted from electronic health records, with treatment response assessed by treating oncologists based on RECIST. $CD4^+$ and $CD8^+$ T-cells were enriched magnetically and analyzed on the IsoLight platform. Single T-cells were captured in microchambers on IsoCode chips for proteomic immune cytokines profiling. Functional polyfunctionality data from 55,775 single cells were analyzed with IsoSpeak software, 2D- and 3D-t-distributed stochastic neighbor embedding (t-SNE) analysis, kappa coefficient, and Kaplan-Meier survival plots. P values ≤0.05 is considered statistically significant.

Results: Pre-treatment baseline polyfunctionality profiles could not differentiate NSCLC patients from healthy subjects, and could not differentiate ICI responders from non-responders. We found a statistically significant difference between responders and non-responders in $CD8^+$ T-cells' changes in overall polyfunctionality (ΔPolyFx) (P=0.01) and polyfunctional strength index (ΔPSI) (P=0.006) in our dynamic pre-/post-treatment single cell measurements, both performing better than PD-L1 TPS alone (P=0.08). In the 3D-t-SNE analysis, subpopulations of post-treatment $CD8^+$ T-cells in ICI responders

displayed distinct immune cytokine profiles from those in pre-treatment cells. $CD8^+$ T-cells ΔPolyFx and ΔPSI scores performed better than PD-L1 TPS in ICI response correlation. Moreover, combined PD-L1 strong TPS and ΔPSI >15 scores strongly correlated with early ICI response with a robust kappa coefficient of 1.0 (P=0.003), which was previously statistically established to indicate a perfect agreement between the prediction and actual response status. Interestingly, high $CD4^+$ T-cells ΔPSI >5 was found to correlate with a strong trend of improved progression-free survival (3.9-fold) (10.8 *vs.* 2.8 months; P=0.07) and overall survival (3-fold) (34.5 *vs.* 11.5 months; P=0.09) in ICI-treated patients.

Conclusions: Our study nominates single peripheral T-cell polyfunctionality dynamics analysis to be a promising liquid biopsy platform to determine potential ICI predictive biomarker in NSCLC. It warrants further studies in larger prospective cohorts to validate the clinical utilities and to further optimize cancer immunotherapy.

Keywords: Cancer immunotherapy; single cell analysis; predictive biomarkers; immune cytokine profiling; polyfunctionality

Submitted Mar 22, 2024. Accepted for publication Aug 23, 2024. Published online Dec 17, 2024.
doi: 10.21037/tlcr-24-260
View this article at: https://dx.doi.org/10.21037/tlcr-24-260

Introduction

The adoption of immune checkpoint inhibitors (ICIs) has transformed lung cancer therapy and favorably impacted the survival outcomes (1). ICIs targeting programmed death-1 (PD-1), e.g., pembrolizumab and nivolumab, and programmed death ligand-1 (PD-L1), e.g., atezolizumab and durvalumab, either alone or in combination with chemotherapy are now standard-of-care regimen for non-small cell lung cancer (NSCLC) (2-5). Currently available ICI predictive biomarkers include (I) PD-L1 tumor proportion score (TPS), (II) tumor mutational burden (TMB) and (III) microsatellite instability (MSI) status (6,7). Nonetheless, a substantial unmet need remains for more reliable and accurate therapeutic predictive biomarkers for optimal patient selection in the use of ICI and emerging novel immunotherapy combinations. Many challenges of ICI clinical use still remain. Given the potential for pseudo-progression in cancer immunotherapy (8), tracking the response profile of ICI therapy can be difficult. Some patients represent late responders (Rs), and the occurrence of immune-related adverse events (irAEs) altogether poses even more obstacles for treatment decision making. The precise role of ICIs in the treatment application for oncogene-addicted NSCLC is also being debated (9-12). Efficacy of ICI treatment of oncogene-addicted NSCLC patients in the setting of acquired targeted kinase inhibitor-resistant progression remains debatable (13,14).

Practical constraints and limitations, including procedure-related risks and limited biopsied-tissues adequacy, hamper the development of tumor tissue-based predictive biomarkers (15,16). These practical factors altogether confound urgent and real-time bedside treatment decisions for advanced NSCLC patients. The development of plasma-based cell-free DNA (cf-DNA) liquid biopsy for molecular profiling has shown to be a desirable alternative to empower personalized cancer therapy (17,18). Recent emerging studies support the potential role of circulating T-lymphocytes as playing critical roles in peripheral recruitment in mounting an immunotherapy treatment response to cancer ICIs (19,20). Of interest, Osorio *et al.* [2019] (20) revealed clinical evidence to support the notion of the recruitment of peripheral T-cells being more critical than reinvigorating exhausted intra-tumoral tumor-infiltrating lymphocytes (TILs) within the lung tumor microenvironment (TME) (21) in the initiation of tumor response towards ICIs. By studying the lesion-level response dynamics to PD-1/PD-L1 ICI treatment in NSCLC, the investigators identified that the response dynamics was characterized by "broad spatial-temporal uniformity", thus favoring a systemic, peripheral recruitment of T-cell response (20). Hence, there is a strong rationale to focus on and characterize the peripheral circulating T-lymphocytes to discover clinically relevant predictive biomarkers of ICI treatment in NSCLC.

State-of-the-art single-cell analysis (22-24) offers advanced opportunities to gain crucial functional insights

into cancer and immune biology that traditional bulk assays cannot match up. The fundamental model of understanding in the human hematopoietic system and its cellular differentiation and diversification serves as the cornerstone to propel the scientific advances in cancer immunotherapy in the past several decades. The immune system is recognized to be highly heterogeneous as an incredibly complex, dynamic, and plastic system. In both physiologic and disease states (such as in cancer and under cancer therapies), highly diverse immune cell types, subtypes, and cell states emerge with distinct underlying functionalities. Traditional marker-based analyses of the immune system in bulk-analytics assays are not able to uncover and address the fundamental questions of rare cells biology and functions inherently responsible for effectuating the immune response. Most recently, single-cell molecular technologies have emerged as invaluable toolsets for further advancing translational insights and clinical applications of cancer immunobiology and therapeutics. In various forms of cancer immunotherapy modalities, including checkpoint inhibitors, the primary antitumoral cytotoxic cellular agents are the T-lymphocytes, specifically $CD8^+$ T-cells. Hence, the ideal ICI predictive biomarkers would likely pertain to measuring the spectrum of antitumor T-cells immune phenotypes, specifically their persistent functionalities over time and immune exhaustion, throughout the course of a patient's ICI treatment regimens. Phenotypic characterization of immune cells, especially various T-cells subtypes have been empowered by emerging single cell methodologies, including high-throughput and multiplexed flow cytometry, as well as single cell genomics and transcriptomic analyses (25). In recent years, applications of single cell-RNA sequencing (scRNA-seq) in the molecular interrogation of the emergence of rare drug-tolerant persister cells under cancer targeted therapy and their relevant cell states in the reprogramming and evolution of precision drug resistance has gained enormous momentum and invaluable insights in the field. However, single cell proteomics analysis to interrogate the immune cellular elements is only in its nascent state, partly due to limitations in functional, protein-level measurements (26). Nonetheless, the question of which T-cell subsets are most relevant in driving ICI treatment response and clinical outcome benefits can only be best deciphered using single cell analysis, preferably with a platform that can empower live functional characterizations. Such a platform could provide unparalleled quantitative assessment of not only the various heterogeneous T-cell subtypes and their differentiation and diversification, but also their functionalities in terms of cytokine secretion and immune modulation and effector functional capacities. These novel single cell methodologies can immensely help to not only enhance deeper understanding of the molecular mechanisms and duration of ICI response, but also mechanisms of ICI resistance emergence as well. Such knowledge base is indispensable to enable better design and treatment management in cancer immunotherapy regimens, patient selection, and treatment monitoring for superior long-term clinical outcomes of the patients.

We hypothesized that dynamic single cell cytokine polyfunctionality profiling of peripheral T-cells in NSCLC patients undergoing ICI immunotherapy can be a novel tool in predicting treatment response and clinical outcome. In this proof-of-concept analysis, we adopted a microfluidics-based multiplexed lab-on-chip proteomics assay platform, IsoLight (Bruker Cellular Analysis, Branford, CT, USA;

Highlight box

Key findings

- Dynamic pre-/post-2 cycles of immune checkpoint inhibitors (ICIs) treatment peripheral single T-cell polyfunctional proteomic cytokine profiling measurements identified a significant difference between responders and non-responders in $CD8^+$ T-cells' changes in overall polyfunctionality (ΔPolyFx) and polyfunctional strength index (ΔPSI).
- In the 3D-t-distributed stochastic neighbor embedding (t-SNE) analysis, there were subpopulations of post-treatment CD8+ T-cells in ICI responders that displayed distinct immune cytokine profiles from those of the pre-treatment cells; which was not evident in the non-responders analysis.
- When combined with programmed death ligand-1 (PD-L1) strong tumor proportion score (TPS), $CD8^+$ T-cells ΔPSI >15 scores strongly correlated with early ICI treatment response with a robust kappa coefficient of 1.0 (P=0.003). High $CD4^+$ T-cells ΔPSI showed correlation with a strong trend of improved progression-free survival (3.9-fold) and overall survival (3-fold) in ICI-treated non-small cell lung cancer (NSCLC) patients.

What is known and what is new?

- PD-L1 TPS has relevant but limited clinical utility as predictive biomarkers in lung cancer ICI immunotherapy.
- Quantitative peripheral live single T-cell dynamic polyfunctionality profiling provides novel and promising methods and indices, ΔPolyFx and ΔPSI, alone or in combination with PD-L1 TPS, to broaden and improve the predictive biomarker repertoire in ICI immunotherapy.

What is the implication, and what should change now?

- Single peripheral T-cell polyfunctionality dynamics analysis could be a promising liquid biopsy profiling platform in NSCLC to determine potential ICI predictive biomarker.

formerly IsoPlexis), to functionally interrogate live peripheral T-lymphocyte subsets at the single-cell level in a discovery study of T-lymphocytes polyfunctionality as a potential predictive biomarker for ICI treatment response and clinical outcomes correlation in NSCLC. This live peripheral single T-cells functional cytokine profiling platform could potentially empower and improve our ability to better interrogate and enhance deep molecular insights into the dynamic heterogeneity of immune cell states and pathways in NSCLC under ICI immunotherapies. We present this article in accordance with the REMARK reporting checklist (available at https://tlcr.amegroups.com/article/view/10.21037/tlcr-24-260/rc).

Methods

Study protocol, patient population, and study procedures

From January 2018 to April 2019, we enrolled patients in an institutional review board (IRB)-approved translational research biorepository study protocol to prospectively collect on-treatment peripheral blood samples longitudinally. The IRB approved the SPECIAL (Serial ProspECtive bIopsy for Appalachian Lung cancer molecular profiling) study protocol (IRB: WVU011117 at West Virginia University, Morgantown, WV, USA). The study was conducted in accordance with the Declaration of Helsinki (as revised in 2013) and informed consent was obtained from all individual participants. Eligible NSCLC patients with histologically confirmed diagnosis for our IsoLight study were selected from a biorepository with adults who underwent PD-1/PD-L1 ICI treatments. No previous therapy with a PD-1 or PD-L1 inhibitor was allowed. Patients with oncogene alterations including *EGFR*, *KRAS* mutations, *MET* amplification or *ALK* translocation were allowed. Molecular alterations of patients were determined under standard-of-care practice of tumoral profiling per treating oncologists and institutional practices. Patients were either treatment naïve or at least 3 weeks out from previous lines of non-ICI systemic lung cancer treatment. Performance status ECOG 0–3 and life expectancy >3 months were required to be included. Healthy donor subjects were collected as controls under IRB-approved protocol (IRB: STUDY00005272 at Penn State Milton S. Hershey Medical Center, Hershey, PA, USA). Demographic and clinical and molecular information, treatment course, and response and survival outcomes information were extracted from the electronic health records (EHR) EPIC, as approved by the IRB protocols. Patients were followed by the treating oncologists under standard clinical care, with response and survival outcomes analyzed based on RECIST criteria and EHR chart review by the study team.

Collection, processing, and selection of T-lymphocytes from peripheral blood samples

Human peripheral blood samples were collected in four ethylenediaminetetraacetic acid (EDTA) tubes at baseline and every two cycles after treatment. Peripheral blood mononuclear cells (PBMCs) were collected by repeated washing in red blood cell (RBC) lysis buffer and cryopreserved in 10% dimethyl sulfoxide (DMSO) in 90% fetal bovine serum (FBS) (Corning, Tewksbury, MA, USA). A portion of the PBMCs were processed for RNA extraction using standard protocols. Cells were thawed according to standard protocols and resuspended in fresh complete RPMI media at 1×10^6/mL and subsequently purified for $CD4^+$ and $CD8^+$ T-lymphocytes using a magnetic bead-based enrichment technique for both $CD4^+$ and $CD8^+$ T-cells (Miltenyi, Gaithersburg, MD, USA). Cells were then stimulated with anti-human-CD3 (10 µg/mL, Cat. No. 16-0037-85, ThermoFisher, Coraopolis, PA, USA) and soluble anti-human-CD28 antibodies (5 µg/mL, Cat. No. 16-0289-81, ThermoFisher) at 37 ℃, 5% CO_2 for 24 hours as previously described (27).

Live T-lymphocytes single cell proteomic cytokines profiling using automated microfluidics lab-on-chip Isolight platform

In our study, we profiled 20 subjects, including ten healthy donors and ten NSCLC patients (*Figure 1*). Patient inclusion in this study is based on chronological protocol enrollment and sample adequacy. Although the cohort size is relatively small, this is a proof-of-concept study with potential advantages of increased assay granularity and increased depth of analysis of biological signals to partially mitigate the aforementioned limitation. Using the IsoLight (Bruker Cellular Analysis; formerly IsoPlexis) proteomic cytokine immune profiling platform, we collected and analyzed single cell data from a total of 55,775 single T-lymphocytes enriched and purified from peripheral blood, including 28,881 $CD4^+$ and 26,894 $CD8^+$ single T-lymphocyte cells. After stimulation for 24 hours, approximately 30,000 cells were loaded onto each proprietary IsoCode chip (Cat. No.

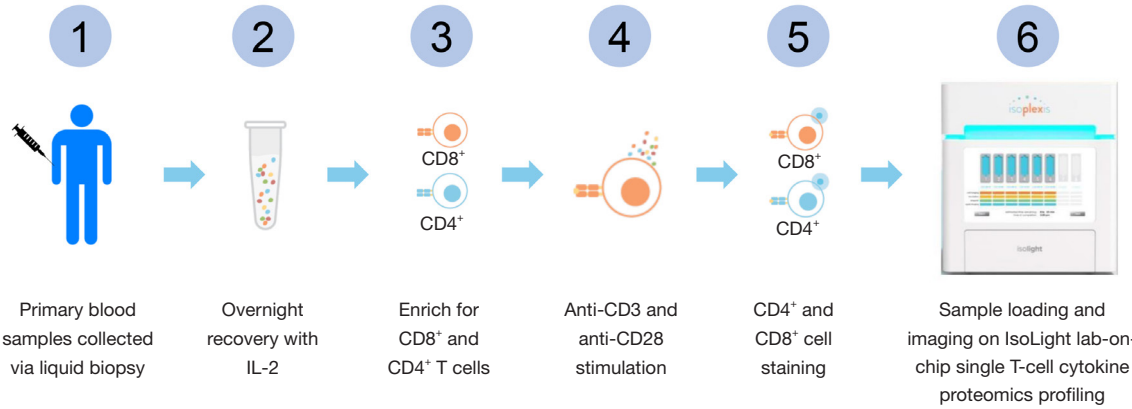

Figure 1 IsoLight single T-cell live functional immune proteomics profiling workflow.

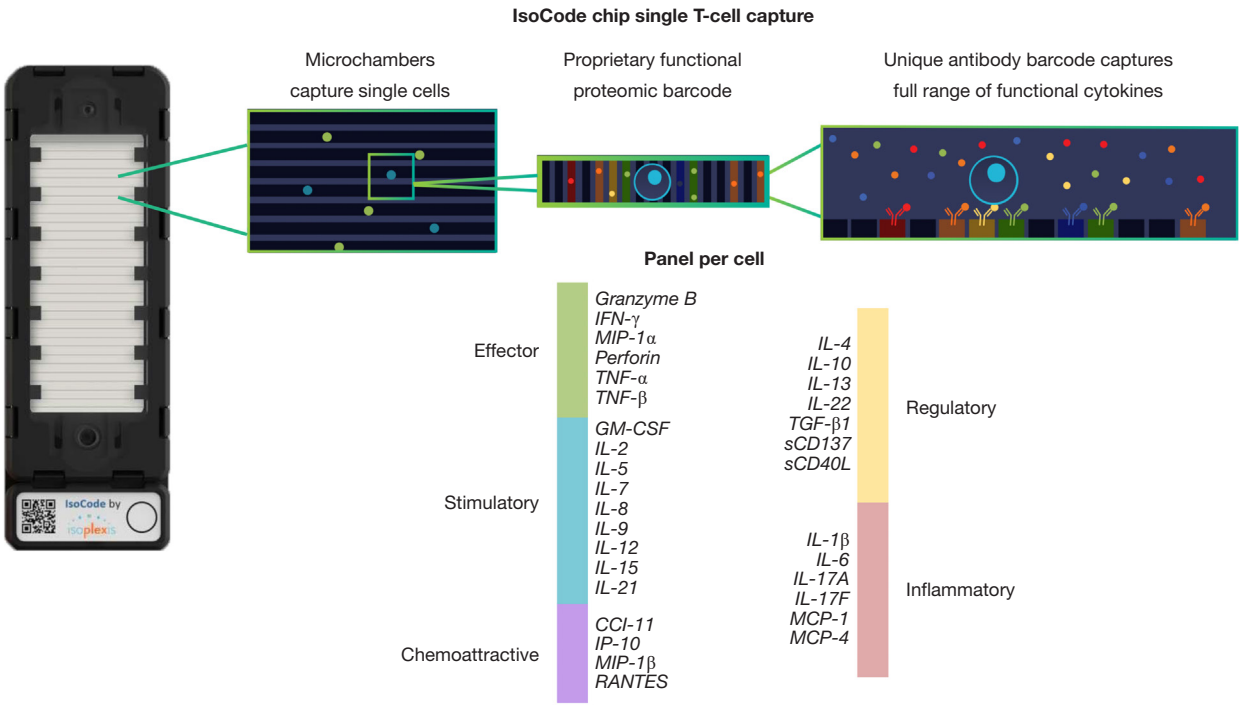

Figure 2 IsoCode chip single T-cell lab-on-chip capture schematic overview. GM-CSF, granulocyte macrophage-colony stimulating factor.

ISOCODE-1001-8, Bruker Cellular Analysis; formerly IsoPlexis). The chips contain ~12,000 microchambers pre-patterned with a 32-plex antibody array, including effector: granzyme B, IFN-γ, MIP-1α, perforin, TNF-α, TNF-β; stimulatory: GM-CSF, IL-2, IL-5, IL-7, IL-8, IL-9, IL-12, IL-15, IL-21; chemoattractive: CCL11, IP-10, MIP-1β, RANTES, IL-4, IL-10, IL-13, IL-22, TGFβ1, sCD137, sCD40L, IL-1β; regulatory: IL-4, IL-10, IL-13, IL-22, TGF-β1, sCD137, sCD40L; and inflammatory: IL-6, IL-17A, IL-17F, MCP-1, MCP-4 (*Figure 2*). Each chip captures between 200–1,500 cells. The cells were then imaged for single cell location in microchambers and incubated at 37 ℃, 5% CO_2 for an additional 16 hours. Following the incubation period, multiplexed enzyme-linked immunosorbent assay (ELISA) detection was used to determine which protein combinations were secreted by each cell. Antibody-barcoded slides captured secreted proteins from single cells; the polyfunctional profile (cells

secreting 2 or more proteins) of single cells was evaluated using the IsoSpeak (Bruker Cellular Analysis; formerly IsoPlexis) bioinformatics software.

Polyfunctional strength index (PSI)

PSI measures highly functional cell subsets capable of secreting multiple cytokines and how intensely those cytokines are being secreted. For PSI, data from empty chambers are used to measure the background level for each protein. These data were used to generate protein abundance histograms, which are fitted by normal distributions and nonparametric methods and judged by goodness of fit. The mean of the histogram identified by the best fit is used as the background level. Single-cell data were then normalized by subtracting this background to compare different samples. Cytokines secreted by less than 2% of the samples were considered non-significantly secreted and excluded from the analysis.

Statistical analysis

Statistical analyses were performed using statistical software R software (R Foundation for Statistical Computing, Vienna, Austria; URL http://www.R-project.org/). Descriptive statistical analyses were performed to summarize the data and to describe the outcome variables including summary tables, proportions, median, and means with standard deviations, scatter-plots and boxplots. Student's *t*-test or Wilcoxon rank test was used in the data analysis on continuous variables, while Chi-squared test was used in categorical variables. Kaplan-Meier method was used in survival analysis. This is hypothesis-generating research and the sample size was not determined from statistical power analysis. In particular, we are developing a proof-of-concept hypothesis-generating model in this pilot study to justify further clinical-translational work. In the bioinformatics analysis, the clustering methods were applied to classify the samples into statistically similar groups and the regression-tree analysis was used to explore and distinguish the samples by the biomarker expression patterns and their differences. Linear model and linear mixed models were used to assess the difference of biomarkers between different groups. The mixed model included different model-parameters with groups as the fixed effect and subjects as random effect. It can handle the repeated measures from the same subjects, taking into account the between-subjects and within-subjects variations. With a similar setting, logistic models and generalized linear mixed models were used to assess binary outcome variables such as a dichotomized biomarker. Analyses were considered statistically significant if $P<0.05$. kappa is a measurement of agreement. The kappa coefficient result is to be interpreted as follows: values 0 as indicating no agreement and 0.01–0.20 as none to slight, 0.21–0.40 as fair, 0.41–0.60 as moderate, 0.61–0.80 as substantial, and 0.81–1.00 as almost perfect agreement (28). Bioinformatics analysis of the polyfunctional profiles of single cells was accomplished using the IsoSpeak (Bruker Cellular Analysis; formerly IsoPlexis) bioinformatics software.

Results

Study cohort and clinical characteristics

The IRB-approved Serial ProspECtive bIopsy for Appalachian Lung cancer molecular profiling (SPECIAL) study was designed to collect serial patient blood samples before and during cancer treatment to empower biomarkers discovery (*Table 1*). Patients diagnosed with NSCLC, either of the adenocarcinoma or squamous cell subtype, both at advanced-stage and recurrent diseases, were included in our study cohort. Peripheral blood samples from healthy donors were also collected as control under IRB-approved protocol. The median age of NSCLC patients was 67 years, while the median age for healthy donors was 60 years. Sixty percent were females in both NSCLC and healthy donor cohorts. Patients were classified as Rs if their tumor assessment showed complete or partial response to treatment according to the RECIST criteria measured two cycles after immunotherapy-based treatments.

Pre-treatment baseline single T-lymphocytes overall polyfunctionality (PolyFx) and PSI: healthy donors versus NSCLC

We first sought to determine if there are differential functions of peripheral circulatory CD4-positive ($CD4^+$) and CD8-positive ($CD8^+$) T-lymphocytes of healthy donors and baseline pre-treatment NSCLC patient samples in our study (*Figure 3*). To this end, we compared their PolyFx and PSI at the single-cell level using the IsoLight and Single-Cell Human Adaptive Immune IsoCode chips (*Figures 1*,*2*). PolyFx is defined as the percentage of single cells secreting two or more cytokines in each sample. In contrast, PSI is defined as the product of multiplying the rate of polyfunctional cells by the average signal intensity of

Table 1 Demographics, clinical and molecular characteristics of the study cohort subjects

Patient ID	Age	Sex	Histology/genotype	TNM stage (8th ed.)	PD-L1 (22C3)	Tx response (s/p 2 cycles)	ICI regimen
0002	66	M	Adenocarcinoma	IIIC (T4N3M0)	90%	SD	Durvalumab
0008	79	M	Adenocarcinoma, MET-amplified	IVB (T4N2M1c)	95%	Excellent PR	Pembrolizumab
0010	68	F	Adenocarcinoma, KRAS-G12C	IVA (T4N2M1a)	60%	Excellent PR	Carbo/Pem/Pembro
0021	71	M	Squamous cell	Recurrence IVA (T4N2M1a)	5%	SD	Pembrolizumab
0024	49	F	Adenocarcinoma, EGFR-del19 (E746_A750del), T790M	IVB (T2N2M1c)	60%	CR	ABCP
0025	66	F	Adenocarcinoma, KRAS-G12C, STK11+, TMB-high (11 muts/Mb)	Recurrence IVA (T1bN2M1b)	<1%	PD	Carbo/Pem/Pembro
0026	57	F	Adenocarcinoma, EGFR-del19 (p.L747_P753 delinsS); PIK3CA-E545K	Recurrence IVA (T3N1M1a)	50%	PD	ABCP
0028	78	M	Adenocarcinoma, ALK-fusion	Recurrence IVA (TxN2M1a)	2%	n/a (alectinib responder)	n/a
0029	60	F	Adenocarcinoma	IVA (T2aN1M1b)	100%	PR (also w/ later Dx of ovarian Ca)	Pembrolizumab
0030	78	F	Adenocarcinoma, KRAS-G12D; PTEN-R130G	IVB (TxN2M1c)	<1%	PD	Carbo/Pem/Pembro
500-096	70	F	Healthy	n/a	n/a	n/a	n/a
500-103	53	F	Healthy	n/a	n/a	n/a	n/a
500-138	53	F	Healthy	n/a	n/a	n/a	n/a
500-282	61	M	Healthy	n/a	n/a	n/a	n/a
500-317	61	M	Healthy	n/a	n/a	n/a	n/a
500-673	62	M	Healthy	n/a	n/a	n/a	n/a
500-887	61	F	Healthy	n/a	n/a	n/a	n/a
500-915	58	F	Healthy	n/a	n/a	n/a	n/a
500-933	61	M	Healthy	n/a	n/a	n/a	n/a
500-996	56	F	Healthy	n/a	n/a	n/a	n/a

M, male; F, female; TMB, tumor mutational burden; muts, mutations; TNM, tumor-node-metastasis; n/a, not available; PD-L1, programmed death ligand-1; Tx, treatment; s/p, status post; SD, stable disease; PR, partial response; CR, complete response; PD, progressive disease; w/, with; Dx, diagnosis; Ca, carcinoma; ICI, immune checkpoint inhibitor; Carbo/Pem/Pembro, carboplatin, pemetrexed, pembrolizumab; ABCP, atezolizumab, bevacizumab, carboplatin, paclitaxel.

significantly secreted cytokines from individual functional groups from each cell. We found that the PolyFx of $CD4^+$ (P=0.23) and $CD8^+$ (P=0.49) T-lymphocytes did not significantly differ between the healthy donor samples and baseline pre-treatment diseased samples (*Figure 3A*,*3B*). There was also no significant difference in the PSI of both $CD4^+$ (P=0.22) and $CD8^+$ (P=0.41) T-lymphocytes (*Figure 3C*,*3D*). We then sought to determine how the healthy donor samples compare to the diseased non-responder (NR) and R samples, respectively (*Figure 3*). The PolyFx of $CD4^+$ (P=0.56) and $CD8^+$ (P=0.49) T-lymphocytes were not significantly different between the healthy donor and the diseased NR samples. The same is true for PSI, where there is no significant difference between $CD4^+$ (P=0.53) and $CD8^+$ (P=0.81) T-lymphocytes when comparing the two sample groups. We also found no

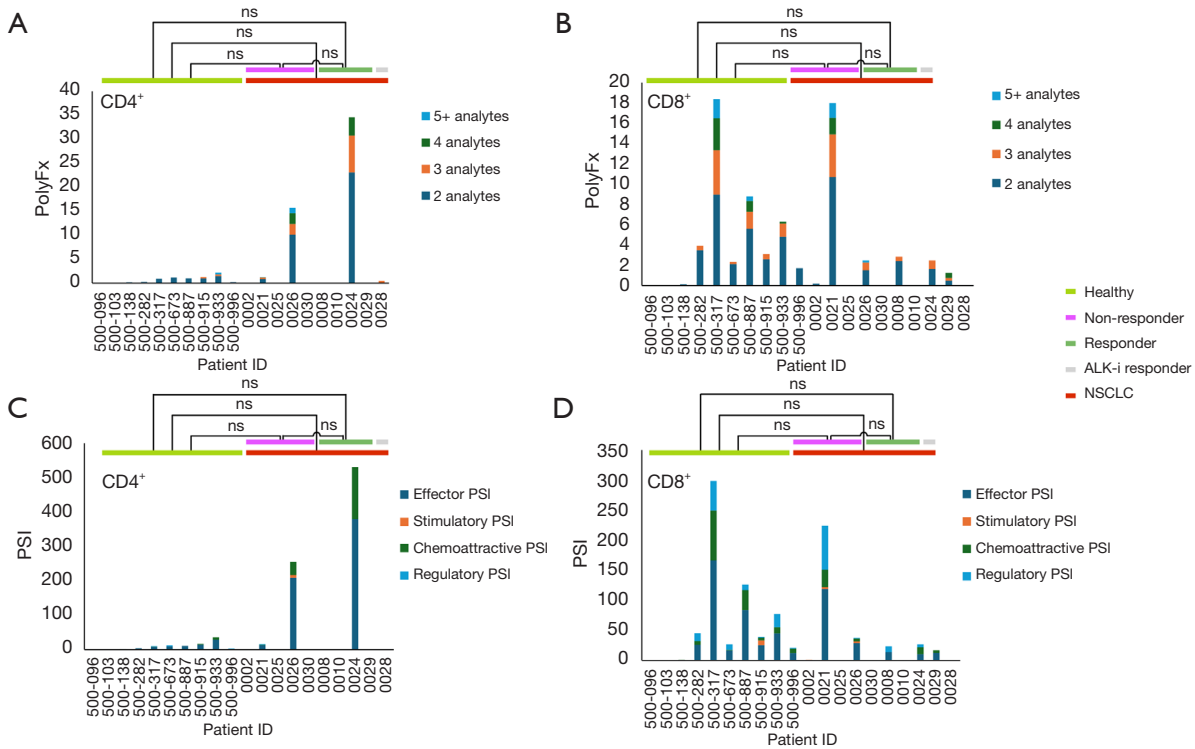

Figure 3 PolyFx and PSI comparison of peripheral single T-cells from healthy donors and pre-treatment baseline blood samples of NSCLC patients. The PolyFx between the healthy donors and the pre-treatment baseline NSCLC patient group was compared for (A) $CD4^+$ T-cells (healthy *vs.* NSCLC, P=0.23; healthy *vs.* non-responder, P=0.56; healthy *vs.* responder, P=0.18) and (B) $CD8^+$ T-cells (healthy *vs.* NSCLC, P=0.49; healthy *vs.* non-responder, P=0.49; healthy *vs.* responder, P=0.32). The PSI between the healthy donors and the pre-treatment baseline NSCLC patient group was compared for (C) $CD4^+$ T-cells (healthy *vs.* NSCLC, P=0.22; healthy *vs.* non-responder, P=0.53; healthy *vs.* responder, P=0.18) and (D) $CD8^+$ T-cells (healthy *vs.* NSCLC, P=0.41; healthy *vs.* non-responder, P=0.81; healthy *vs.* responder, P=0.28). Statistical analysis was performed with a Wilcoxon rank test. PolyFx, overall polyfunctionality; PSI, polyfunctional strength index; NSCLC, non-small cell lung cancer; ns, not significant (P>0.05); ALK; anaplastic lymphoma kinase; ALK-i, ALK inhibitor.

significant difference in PolyFx between the healthy donor samples and the diseased R samples for $CD4^+$ (P=0.18) and $CD8^+$ (P=0.32) T-lymphocytes. The PSI between these two sample groups showed no significant difference in $CD4^+$ (P=0.18) and $CD8^+$ (P=0.28) T-lymphocytes. Our results are consistent with high immune functional heterogeneity among the NSCLC patients' pre-treatment baseline T-lymphocytes prior to ICI treatment initiation.

Next, we sought to determine, among the NSCLC patients, the correlation between the pre-treatment baseline PolyFx or PSI from $CD4^+$, $CD8^+$, and total ($CD4^+$ and $CD8^+$) T-lymphocytes and ICI early treatment response (*Figure 3*; Figure S1A). There were no statistically different baseline PolyFx or PSI values between ICI Rs and NRs (P>0.05). This is true for $CD4^+$, $CD8^+$ alone (*Figure 3*), or combined total T-lymphocytes (Figure S1A). Here, our data suggest that baseline pre-treatment single T-cell polyfunctionality or PSI alone at a single time point assay from NSCLC patients under ICI treatment (with or without chemotherapy) was inadequate to predict ICI treatment response.

Early changes in peripheral $CD8^+$ T-lymphocytes single cell overall polyfunctionality (ΔPolyFx) and PSI (ΔPSI) as novel predictors of ICI treatment response

Next, we sought to determine the single T-lymphocyte early onset longitudinal changes in overall polyfunctionality (ΔPolyFx) between baseline pre-treatment T-lymphocytes and those collected after two cycles of ICI treatments (post-treatment) (*Figure 4*). For $CD4^+$ T-lymphocytes, there was no significant difference in ΔPolyFx between the ICI NR group and the R group (*Figure 4A*: P=0.81, Wilcoxon rank test; *Figure 4E*: P=0.64, mixed model). On the other

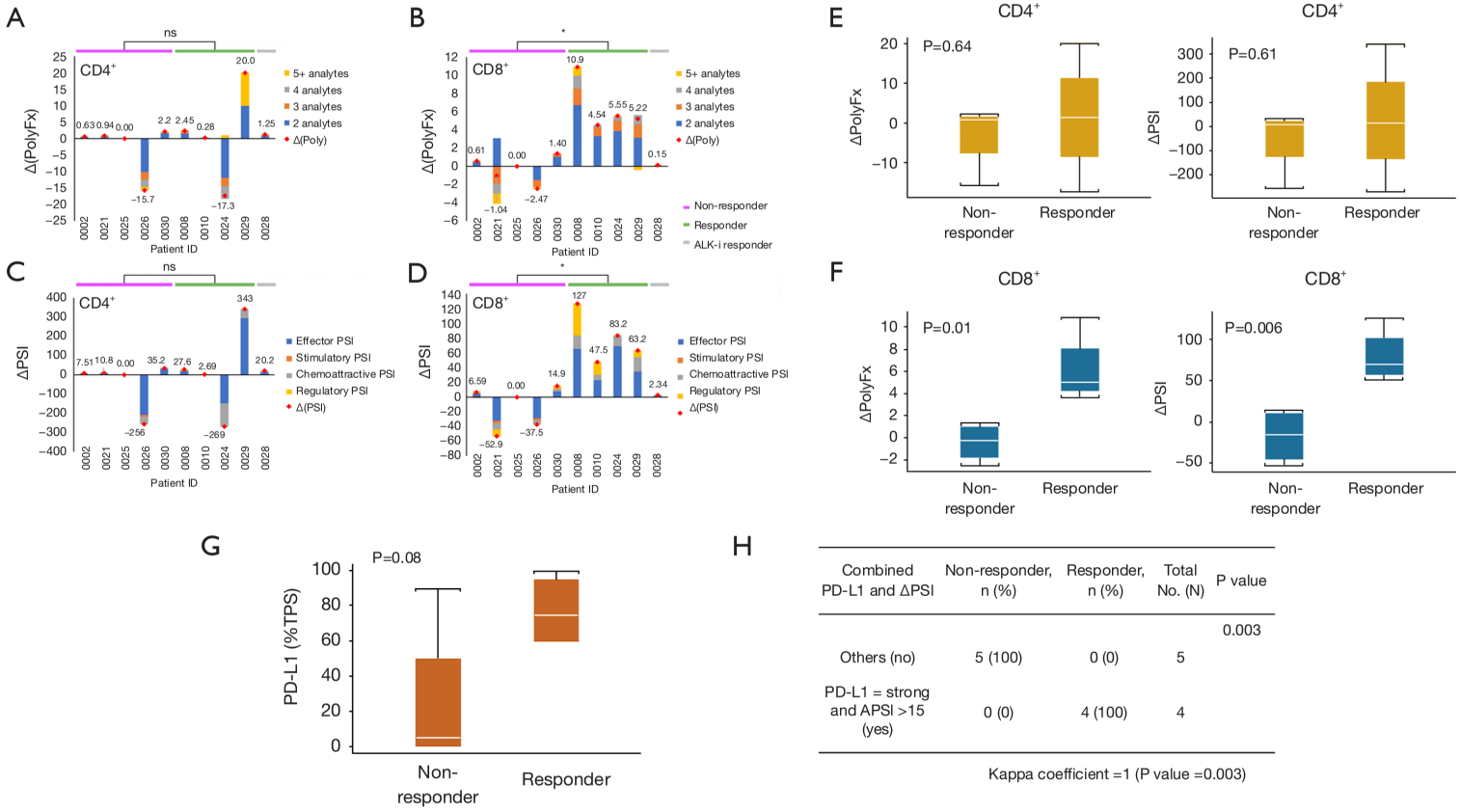

Combined PD-L1 and ΔPSI	Non-responder, n (%)	Responder, n (%)	Total No. (N)	P value
				0.003
Others (no)	5 (100)	0 (0)	5	
PD-L1 = strong and APSI >15 (yes)	0 (0)	4 (100)	4	

Kappa coefficient =1 (P value =0.003)

Figure 4 Comparing the changes in PolyFx and PSI after two cycles of ICI treatment in responders *vs.* non-responders. The ΔPolyFx between responders and the non-responders were compared for (A) $CD4^+$ T-cells (P=0.81) and (B) $CD8^+$ T-cells (P=0.02). The ΔPSI between the responders and non-responders were compared for (C) $CD4^+$ T-cells (P=0.91) and (D) $CD8^+$ T-cells (P=0.02). Statistical analysis was performed with Wilcoxon rank test. Whisker plots representing the ΔPolyFx and ΔPSI in responders *vs.* non-responders in (E) $CD4^+$ T-cells and (F) $CD8^+$ T-cells revealing a significant difference between responders and non-responders in CD8+ T-cells. Statistical analysis was performed using a mixed model. (G) Comparing the TPS for tumoral PD-L1 expression between responders and non-responders revealed that there is no significant difference (P>0.05) between the two groups. (H) Combining PD-L1 strong TPS and $CD8^+$ ΔPSI >15 strongly predicts early ICI treatment response to immunotherapy with a kappa coefficient of 1.0 (P=0.003). *, significant (P<0.05). PSI, polyfunctional strength index; PolyFx, overall polyfunctionality; ΔPSI, change in PSI; ΔPolyFx, change in PolyFx; ns, not significant (P>0.05); ALK-i, ALK inhibitor; PD-L1, programmed death ligand-1; ICI, immune checkpoint inhibitor; TPS, tumor proportion score.

hand, for $CD8^+$ T-lymphocytes, we observed a statistically significant difference in ΔPolyFx when comparing the NR group to the R group (*Figure 4B*: P=0.02, Wilcoxon rank test; *Figure 4F*: P=0.01, mixed model). When examining the changes in polyfunctionality strength index (ΔPSI), we observed no significant difference in $CD4^+$ ΔPSI (*Figure 4C*: P=0.91, Wilcoxon rank test; *Figure 4E*: P=0.61, mixed model) between the ICI R and NR groups. For $CD8^+$ ΔPSI, however, we observed a statistically significant difference of ΔPSI between the R and NR groups (*Figure 4D*: P=0.02, Wilcoxon rank test; *Figure 4F*: P=0.006, mixed model). When $CD4^+$ ΔPSI was added to $CD8^+$ ΔPSI in the combined total T-lymphocytes ($CD4^+$/$CD8^+$) analysis, the statistical difference between the R and NR groups became diminished (P=0.19, Figure S1B). Our study results nominate ΔPolyFx and ΔPSI of $CD8^+$ T-lymphocytes as a potential predictive biomarker of ICI treatment response in NSCLC.

$CD8^+$ ΔPolyFx and ΔPSI perform better than PD-L1 TPS alone as a predictive biomarker for ICI treatment response in NSCLC

In our study cohort, we also asked if the early changes in polyfunctional strength could be a stronger predictor of early ICI treatment response compared to PD-L1 TPS. The patient's tumoral PD-L1 TPS expression status alone failed to correlate with statistical significance with early ICI treatment response (P=0.08) (*Figure 4G*). As above, both the $CD8^+$ ΔPolyFx and ΔPSI perform better than PD-L1 TPS alone as a predictive biomarker significantly correlated with NSCLC ICI treatment response (*Figure 4F*). Next, we performed a combined analysis of the $CD8^+$ ΔPSI and PD-L1 TPS status as potential predictors of treatment response under ICI-based treatment. Our results show that a combined $CD8^+$ ΔPSI >15 and PD-L1 strong TPS status analysis significantly and robustly correlated with ICI treatment response with a kappa coefficient of 1.0 (P=0.003), indicating both a sensitivity and specificity of 100% (*Figure 4H*).

2D t-distributed stochastic neighbor embedding (t-SNE) and 3D t-SNE bioinformatics analysis of R and NR treatment response groups

To further illustrate the difference in polyfunctional strength change between R and NR groups, as well as the cellular heterogeneity among cells of the same sample, we generated 2D t-SNE plots based on the intensity of cytokines secreted per cell for both $CD4^+$ and $CD8^+$ T-lymphocytes. The 2D t-SNE plots of both $CD4^+$ and $CD8^+$ T-lymphocytes for a representative NR (Patient-0002) and R (Patient-0008) were shown here (*Figure 5A,5B*). The 2D t-SNE plots corroborated the observation that the change in polyfunctional strength separating Rs from NRs was more pronounced in $CD8^+$ T-lymphocytes. Our results demonstrate that the increase in cytokines secreted between pre-treatment and post-treatment samples was more prominent in $CD8^+$ T-lymphocytes but less so in $CD4^+$ T-lymphocytes. The plots also illustrated the heterogeneity in the intensity of cytokines secreted between single cells in the same sample, highlighting the importance of single polyfunctional cells in ICI response.

Additionally, we represented the polyfunctionality data as heat maps with the contributions of each group of cytokines to the PolyFx or PSI listed. Patient-0002 (NR) and Patient-0008 (R) were shown here with heat maps generated based on $CD8^+$ (*Figure 5C,5D*) and $CD4^+$ (*Figure 5E,5F*) T-cells PSI and PolyFx as representative illustrations. The percentage of $CD8^+$ T-cells with high average PSI increased for the R after ICI treatment, primarily driven by single cells secreting sCD137, granzyme B, and IFN-γ (*Figure 5C*). In contrast, for the NR, the increase was not observed, reflecting what was described in the total change in PSI. Likewise, the percentage of highly polyfunctional $CD8^+$ T-cells in R was also induced after treatment, while being less so for NR (*Figure 5D*). The changes pre- and post-treatment were not as highly discernible for $CD4^+$ T-cells, partly due to the low number of significantly secreted cytokines.

Next, we performed a $CD8^+$ 3D t-SNE plot analysis of the NR and R groups pre- and post-treatment (two cycles of ICI) (*Figure 5G,5H*). Our study results showed that there were distinct subpopulations of post-treatment $CD8^+$ T-cells found to be segregated from the pre-treatment cells in the ICI R (*Figure 5H*) at the single cell level but not evident among the ICI NR (*Figure 5G*), suggesting that $CD8^+$ T-cells secreted cytokines can delineate between the R and NR groups at the single-cell level. This further corroborates our hypothesis to nominate functional single-cell analysis of peripheral $CD8^+$ T-cells as a predictive biomarker of ICI early treatment response.

ΔPSI in predicting treatment response of oncogene-addicted NSCLC under targeted therapies versus ICI therapy

Oncogene-addicted lung cancers generally respond

Figure 5 2D and 3D t-SNE plots reveal greater upregulation of PolyFx and PSI in CD8$^+$ T-cells. All single cells secreting the indicated cytokines and the intensity of cytokines secreted between a representative non-responder (Patient-0002) and a representative responder (Patient-0008) pre- and post-two cycles of ICI therapy were visualized using a 2D t-SNE plot for (A) CD4$^+$ T-cells and (B) CD8$^+$ T-cells. Each dot represents a single cell. The parameters used for generating the 2D t-SNE plot are as follows: iterations =3,000, perplexity =50. The heat maps reveal greater upregulation of polyfunctional subpopulations with unique cytokine signatures in CD8$^+$ T-cells both when sorted by (C) average PSI and (D) PolyFx from responders (as in Patient-0008) compared with non-responders (as in Patient-0002), but not so in CD4$^+$ T-cells when sorted by (E) average PSI and (F) PolyFx. (G) The 3D t-SNE plot of pre- and post-treatment CD8$^+$ T-cell subsets in non-responders revealed considerable overlap between the two early treatment time points (with the intervals between cycle one and two of ICI), suggesting no appreciable difference between the profiles of cytokines secreted before and after ICI treatment. The dotted orange and blue circles illustrate the profile boundaries of each cell cluster. The parameters used for this plot were as follows: iterations =3,000, perplexity =100. (H) The 3D t-SNE plot of pre-and post-treatment CD8$^+$ T-cell subsets in responders revealed that the two on ICI-treatment samples tend to form distinct clusters of cytokine immune profiles. The dotted orange and blue circles illustrate the profile boundaries of each cell cluster. The parameters used for this plot were as follows: iterations =3,000, perplexity =100. ICI, immune checkpoint inhibitor; NR, non-responder; R, responder; t-SNE, t-distributed stochastic neighbor embedding; PSI, polyfunctional strength index; PolyFx, overall polyfunctionality; NR, non-responder; R, responder.

unfavorably to ICI treatments, especially in first-line setting (10,29,30). The value of ICIs as further lines of salvage treatment in the acquired tyrosine kinase inhibitor (TKI) drug resistance setting remains controversial (9,31). Here, we sought to determine the predictive value of ΔPSI in the oncogene-addicted NSCLC patients in our study cohort under various therapeutic modalities.

Patient-0008 is a 79-year-old male, active smoker with 120 pack-years cigarette smoking history and ongoing pipe smoking habit at time of diagnosis. He presented with *TP53* mutation and *MET* genomic amplification-positive metastatic poorly differentiated lung adenocarcinoma, stage IVB (cTxN2M1c), with metastasis to his brain and right adrenal gland at time of initial diagnosis. His tumoral PD-L1 TPS was 95% (22C3). He was initially treated with the anti-PD-1 ICI pembrolizumab alone as his first-line therapy, and experienced near complete response after two cycles. His $CD8^+$ T-cell ΔPolyFx was 10.9 and ΔPSI 127 (*Figure 4B*,*4D*), both correlating well with his ICI treatment response status as an R.

Patient-0024 is a 49-year-old, never-smoker woman who had recurrent *EGFR* exon 19 deletion (E746_A750del) driven lung adenocarcinoma after prior lobectomy and subsequent chemoradiotherapy for recurrence. She was sequentially treated with erlotinib followed later by osimertinib both with favorable durable near complete response profile under respective TKIs. Eventually, she was treated with the atezolizumab, bevacizumab, carboplatin, paclitaxel (ABCP) regimen after acquired osimertinib-resistant progression (14,32). The tumoral PD-L1 expression was strong (TPS 60%; 22C3). She experienced both complete tumor response and metabolic response upon initial ABCP treatment. Her $CD8^+$ T-cell ΔPolyFx was 5.55 and ΔPSI 83.2 (*Figure 4B*,*4D*), which correlated well with her ICI treatment response status as a R. She completed a total of four cycles of the ABCP induction treatment regimen, with ongoing favorable tumor response on maintenance bevacizumab-atezolizumab therapy.

Patient-0026 is a 57-year-old woman, never-smoker, who had *EGFR* exon 19 deletion (L747_P753 delinsS)-driven metastatic lung adenocarcinoma that ultimately progressed on erlotinib in acquired drug resistance despite initial tumor response. She was then treated with the ABCP regimen as second-line therapy. She had a strong tumoral PD-L1 expression level, with TPS being 50% (22C3). Restaging imaging studies confirmed non-response status with a mixed early response profile, with refractory progressive disease in the right upper lobe apical nodular opacities despite thoracic nodal adenopathy reduction in her mediastinal and right hilar nodes. Her $CD8^+$ T-cell ΔPolyFx and ΔPSI was found to be −2.47 and −37.5 respectively (*Figure 4B*,*4D*), accurately predicting her as an ICI NR despite the strong PD-L1 expression.

Patient-0028 is a 78-year-old male, former smoker, who had *ALK*-translocation-driven recurrent advanced NSCLC and was treated with the ALK-TKI alectinib. He responded remarkably to alectinib as expected. Little is known regarding any potential role of a patient's innate immune response in contributing to tumor response under targeted therapy. Here, we found that Patient-0028 had his $CD4^+$ and $CD8^+$ ΔPSI scores correlate only weakly to his response status (*Figure 4B*,*4D*). His tumoral PD-L1 TPS was 2% (22C3). Taken together, our data suggests that although ΔPolyFx and ΔPSI can predict early ICI treatment response in oncogene-addicted NSCLC, it is not likely to be applicable for treatment under molecular targeted inhibitors.

Longitudinal monitoring of ICI treatment response using peripheral single cell T-lymphocytes proteomic cytokines profiling on treatment

Here, we further studied three particular patients in our pilot study cohort, i.e., NR: Patient-0002; and Rs: Patient-0008, and Patient-0024, to derive more insights into their on-treatment longitudinal landscapes of T-cell PolyFx and PSI. Our study results showed that the longitudinal $CD8^+$ T-cell PSI profiles in Rs displayed association with the treatment response profile (*Figure 6A*,*6B*) but less so in the NR (*Figure 6C*). For the NR Patient-0002, the PolyFx and PSI only minimally increased after two cycles of ICI. Both the PolyFx and PSI exhibited further increase upon seven more cycles of ICI when the patient experienced on-treatment stable disease according to CT imaging. The PolyFx and PSI decreased after four more cycles of ICI when the patient remained in persistent stable disease status.

For the Rs Patient-0008 (*Figure 6A*) and Patient-0024 (*Figure 6B*), the PolyFx and PSI increased significantly after two cycles of ICI treatment, confirming that ICI treatment response correlated with an increase in PolyFx and PSI after two cycles. Both patients showed correlating decline in both PolyFx and PSI at time of disease progression as per body imaging diagnosis. Patient-0008 further underwent MET-targeted therapy CBT-101 (i.e., APL-101) and crizotinib after initial ICI treatment, given his molecular findings of

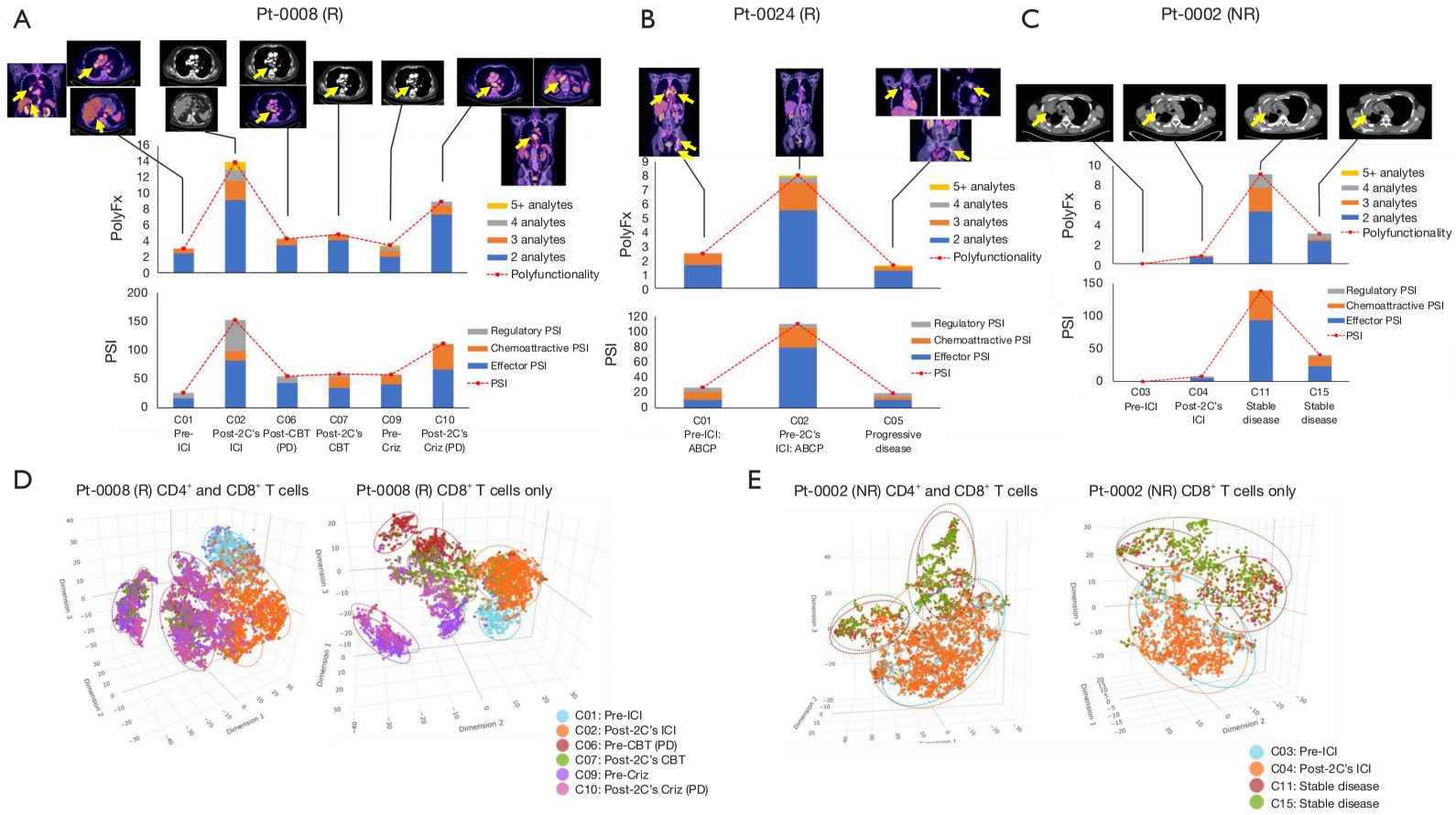

Figure 6 Longitudinal profiles of the CD8$^+$ T-cell PolyFx and PSI alterations of NSCLC patients undergoing ICI-based treatment and further lines of cancer therapies. Patients-0002, –0008, and –0024 were followed longitudinally, and their PolyFx and PSI dynamic landscapes were plotted and schematically represented here. Key correlating clinical imaging scans were included and presented for illustrative purposes. (A) Responder Patient-0008. A 79-year-old male, active smoker with 120 pack-years cigarette smoking history and ongoing pipe smoking habit, with *TP53* mutation and *MET* genomic amplification positive metastatic poorly differentiated lung adenocarcinoma, stage IVB (cTxN2M1c), with metastasis to his brain and right adrenal at time of initial diagnosis. His tumoral PD-L1 TPS was 95% (22C3). He initially presented with mental status change and a motor vehicle accident when it was found, in the emergency department, that he had an abnormal 1.5 cm × 1.5 cm × 2 cm ring-enhancing left frontal mass metastasis with extensive vasogenic edema with subfalcine herniation and effacement of the left lateral ventricle. He was initially treated with gamma knife radiotherapy and then systemic pembrolizumab 200 mg IV every three weeks ICI alone as his first-line therapy, and experienced near complete response after two cycles. He later had repeat brain gamma knife radiotherapy for a new subcentimeter brain metastasis, with continuation of ICI afterwards with continual near complete response status. His CD8$^+$ T-cell ΔPolyFx was 10.9 and ΔPSI was 127 (*Figure 4B,4D*), both correlating well with his ICI treatment response status as a responder. Disease progression was noted in July 2018, after ten cycles of pembrolizumab, with enlargement of subcarinal lymph node (confirmed by positive rebiopsy), and enlarging paratracheal mediastinal nodes and intraabdominal adenopathy. He was then enrolled in a phase 1 clinical trial study treatment using a MET inhibitor CBT-101 with partial response after two cycles of treatment. However, he withdrew from study

treatment thereafter due to his concern for treatment-related adverse effects, declining the offer of a trial dose reduction. He was switched to another MET inhibitor crizotinib in December 2018, with which he achieved stable disease response on a total of about two months' therapy with subsequent discontinuation due to intolerance. He was found to be on disease progression, confirmed by PET/CT imaging eventually in April 2019, with significant weight loss, abdominal pain, and hyperbilirubinemia with clinical jaundice. He was admitted to the hospital and ultimately enrolled in hospice care. Yellow arrows on the imaging scans indicate tumor disease burden. (B) Responder Patient-0024. A 49-year-old, never-smoker woman who had recurrent *EGFR* del19 (E746_A750del)-driven lung adenocarcinoma after prior lobectomy and subsequent chemoradiotherapy for recurrence. She then presented with mental status change in recurrence due to brain metastases, which was treated with craniotomy and gamma knife radiotherapy. She was initially started on erlotinib with best complete response, but was later found to have widespread progression on erlotinib and was switched to osimertinib (due to emergence of acquired *EGFR*-E746_A750del + T790M mutation in erlotinib acquired resistance), with essential complete response. Eventually, she was treated with ABCP after osimertinib-resistant progression. The tumoral PD-L1 expression was strong (TPS 60%; 22C3). Intriguingly, she experienced both complete tumor response and metabolic response after merely just one cycle of the ABCP treatment, despite treatment toxicities delaying her 2nd cycle of treatment to 6 weeks later. Her CD8^{+} T-cell ΔPolyFx was 5.55 and ΔPSI was 83.2 (*Figure 4B,4D*), which correlated well with her ICI treatment response status as a responder. She then continued to complete a total of four cycles of the ABCP induction combination therapies, with continual response on extended maintenance bevacizumab-atezolizumab therapy. Yellow arrows on the imaging scans indicate tumor disease burden. (C) Non-responder Patient-0002. A 66-year-old male, active smoker of 22.5 pack-years history who presented with a worsening productive cough over four months, along with dyspnea, anorexia, and weight loss of 10 pounds, and post-obstructive pneumonia of his right lung. CT chest and PET/CT imaging eventually confirmed a bulky 12 cm × 10 cm right upper lobe apical mass with mediastinal adenopathy, with the largest being 2.7 cm in the aorta-pulmonary window. CT-guided biopsy of the right lung mass confirmed a poorly differentiated adenocarcinoma. PD-L1 expression was strong at TPS 90% (22C3). There was left supraclavicular hypermetabolic adenopathy in addition to the right hilar and mediastinal disease involvement. He was started on concurrent chemoradiotherapy with cisplatin and etoposide; and later treated with the anti-PD-L1 ICI durvalumab in early 2018, which showed the best response as a stable disease after a total of 12 months of the ICI treatment. Yellow arrows on the imaging scans indicate tumor disease burden. (D) 3D t-SNE plots of longitudinal treatment time points in a representative responder Patient-0008. Patient-0008's pre- and post-2 cycles ICI single cell populations segregated away from each other, coinciding with his status as an ICI treatment responder. The C06, C07, C09, and C10 time points clustered further away after the early tumor ICI treatment response, coinciding with the time when the tumor began to progress. When the patient underwent further non-ICI *MET*-targeted therapy treatment regimens (CBT-101 and crizotinib), the single cells clustered away from when the patient underwent ICI treatment, showing that our live functional T-cell measurement is sensitive enough to detect the difference in peripheral T-cells immune functionality landscapes during the evolving course of cancer treatment modalities and disease burden changes. (E) 3D t-SNE plots of longitudinal treatment time points in a representative non-responder Patient-0002. Patient-0002's non-responder status was reflected in the longitudinal 3D t-SNE plot as single cells clustering close to each other in the pre-and post-2 cycles of ICI treatment samples (dotted orange and blue circles). The stable disease and persistent stable disease single T-cell samples evidently displayed some clustering away from the pre- and post-treatment samples, suggesting potential tumor microenvironment influence and evolving single T-cell functional flux alterations within stable disease status. PSI, polyfunctional strength index; PolyFx, overall polyfunctionality; ICI, immune checkpoint inhibitor; 2C, 2 cycles; CBT, CBT-101 MET tyrosine kinase inhibitor; PD, progressive disease; Criz, crizotinib; ABCP, atezolizumab, bevacizumab, carboplatin, paclitaxel; NR, non-responder; R, responder; NSCLC, non-small cell lung cancer; PD-L1, programmed death ligand-1; TPS, tumor proportion score; IV, intravenous; ΔPSI, change in PSI; ΔPolyFx, change in PolyFx; PET, positron emission tomography; CT, computed tomography; t-SNE, t-distributed stochastic neighbor embedding.

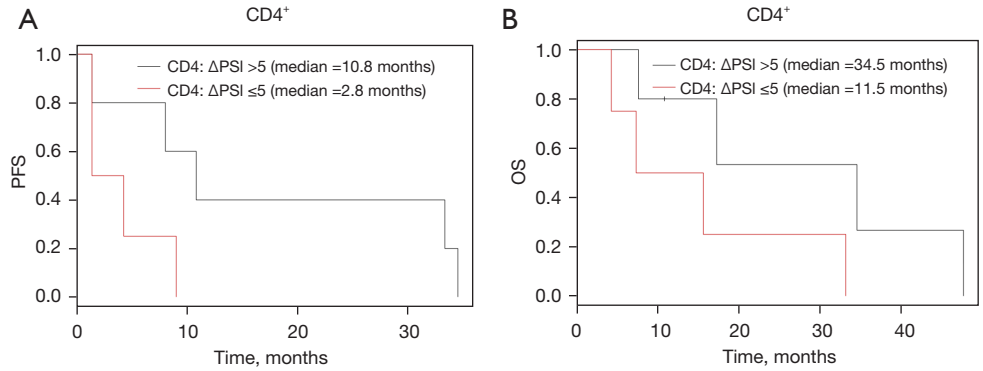

Figure 7 Kaplan-Meier clinical survival outcomes analysis of PSI changes (ΔPSI) in ICI-treated NSCLC. CD4+ T-cells analysis. (A) The median PFS of patients with CD4+ ΔPSI >5 was 10.8 months, whereas those with ΔPSI ≤5 has median PFS of 2.8 months, with a 3.9-fold difference (P=0.07). (B) The median OS of patients with CD4+ ΔPSI >5 was 34.5 months, whereas those with ΔPSI ≤5 has median PFS of 11.5 months, with a 3-fold difference (P=0.09). PFS, progression-free survival; OS, overall survival; PSI, polyfunctional strength index; ΔPSI, change in PSI; ICI, immune checkpoint inhibitor; NSCLC, non-small cell lung cancer.

MET genomic amplification status. Nonetheless, his PolyFx and PSI remained low throughout the targeted therapy time points with best stable response on MET-TKIs. Overall, a decline in the CD8+ T-cell PSI on and during ICI treatment beyond cycle two may predict emerging progressive disease and resistance against ongoing ICI-based therapy.

When we analyzed the single CD8+ T-cells in 3D t-SNE plots, we observed that for the R: Patient-0008, the post-treatment CD8+ T-cells segregated meaningfully from the baseline pre-treatment cells (*Figure 6D*). These results suggest that the circulating T-cells under ICI treatment are functionally distinct and discernible from baseline T-cells. For Patient-0008, the progression and MET-targeted inhibitor treatment time points were segregated further away from the pre- and post-treatment samples, indicating that when the tumor progressed, there were observable differences in the functionality of the respective T-cells. On the other hand, for the NR: Patient-0002, the pre-treatment cells were not distinguishable from the post-2 cycles treatment cells (*Figure 6E*). In Patient-0002, the stable disease (C11) and persistent stable disease (C15) time points appear to segregate apart from the pre-and post-treatment samples, implying that the T-cells in these time points may also possess differential functionality profiles.

Kaplan-Meier clinical survival outcomes analysis

Lastly, we performed Kaplan-Meier survival analysis on our study cohort to better understand the impact of the longitudinal single T-cells interrogation on long-term survival outcomes in addition to early ICI treatment response. Intriguingly, our data showed that a high change in CD4+ PSI (ΔPSI >5) after ICI treatment had a longer median progression-free survival (PFS) of 10.8 months compared with that of 2.8 months otherwise. The Kaplan-Meier survival analysis showed that patients with a high CD4+ ΔPSI >5 were correlated with a strong trend of improved PFS, with a nearly four-fold (3.9) longer PFS than those with a low CD4+ ΔPSI (P=0.07) (*Figure 7A*). Similarly, patients with a high CD4+ ΔPSI also were correlated with a strong trend of improved median overall survival (OS), with a three-fold (3.0) longer OS than those with a low CD4+ ΔPSI (34.5 *vs.* 11.5 months; P=0.09) (*Figure 7B*).

Discussion

ICI using anti-PD-1/PD-L1 antibodies alone or in combination with chemotherapy has become standard-of-care for not only advanced metastatic stage NSCLC but also early resectable stage patients in the form of adjuvant (IMpower-010) (33), neoadjuvant (CheckMate-816) (34) and perioperative chemoimmunotherapy (Keynote-617) (35). Nonetheless, there remains an unmet need for robust predictive immunotherapy biomarkers to best select patients for treatment and to guide optimal therapeutic strategies. Currently available biomarkers for ICI treatment, e.g., PD-L1 expression, MSI status, and TMB, often experience limitations in predictive capability especially when an ICI is combined with chemotherapeutics (34-38). Our study here provided proof-of-concept evidence to support the

development of liquid biopsy-based live peripheral single T-cell cytokine proteomics profiling as an ICI treatment predictive biomarker platform in lung cancer. We showed that the longitudinal peripheral $CD8^+$ T-lymphocytes PSI profile, as measured in ΔPSI score under ICI immunotherapy, performs better than PD-L1 TPS alone as a potential predictive biomarker for ICI treatment response. Importantly, our study showed that combining $CD8^+$ ΔPSI >15 and PD-L1 strong TPS status as a predictive biomarker significantly correlated with ICI-based treatment response with a robust kappa coefficient of 1.0 (P=0.003). Additionally, $CD4^+$ T-lymphocytes ΔPSI >5 correlated with a strong trend of both improved PFS (~4-fold) and OS (3-fold) in our current study.

Emerging blood-based predictive and prognostic biomarkers under investigations in the form of liquid biopsy offer considerable advantages over the reliance on tumor-tissue-based biomarker assays (39-41). Our study now nominates a real-time longitudinal liquid biopsy assay to predict ICI therapeutic response and long-term clinical survival outcomes by quantifying the intensity profiles of different cytokines released by peripheral $CD4^+$ and $CD8^+$ T-cells before and during treatment into a functional score. In our patient cohort, PD-L1 TPS as a predictive biomarker for ICI treatment tumor response was determined to be only at 80% accuracy. On the other hand, ΔPSI in $CD8^+$ T-lymphocytes alone could significantly distinguish between ICI Rs and NRs (P=0.006, mixed model). When combining PD-L1 TPS with ΔPSI, the integrated ΔPSI/PD-L1 TPS biomarker strategy predicted tumor response with 100% accuracy (*Figure 4H*, P=0.003). Notably, the immune treatment response to anti-PD-1/PD-L1 ICI in cancer patients can be highly heterogeneous (22). Published studies have shown that the presence of rare, highly functional cells is important in predicting the overall response of the population (19,27,42). Population-based techniques such as bulk ELISA and flow cytometry merely provide an aggregated view of all the cells that comprise a population, which masks the contribution of the polyfunctional super-cytokine secretory cells. On the other hand, single-cell methods have been shown to retain critically important cellular elements and differences in the immune cell compartments. As such, single-cell methods prove to be more advantageous when determining therapeutic response driven by rare, highly polyfunctional immune cells in the setting of ICI response, and similarly when considering ICI treatment-acquired resistance.

Our study also promises to provide further utility in uncovering the dynamic changes in functionality landscapes in longitudinal on-treatment immune cells. By analyzing the ΔPSI in peripheral single T-cells at set intervals during an ICI-based treatment course, our liquid biopsy method identified a promising trend of single T-cell functionality changes correlating with emerging ICI treatment resistance, which may ultimately lead to better treatment decisions. We presented the 3D t-SNE plots of longitudinal treatment time points in representative ICI NR Patient-0002 and R Patient-0008. Despite expressing high PD-L1, Patient-0002's T-cells clustered close to each other in the pre-and post-2 cycles of ICI samples. Intriguingly, the longitudinal additional time-point of "stable disease" (C11) and "persistent stable disease" (C15) samples clustered away from the pre- and post-treatment (C03 and C04) samples, suggesting that the tumor microenvironment may be changing under ICI treatment pressure. Further studies focusing on immune cellular functionality landscapes in radiographic stable disease status are warranted. To this end, our liquid biopsy methodology offers the opportunity to better interrogate the functionality of the T-cells, thereby enabling us to track with higher fidelity the underlying metabolic and molecular responses not always fully represented by CT radiographic measurements *per se*. In contrast, Patient-0008, who had *MET* amplification and was an ICI treatment R, had ΔPolyFx and ΔPSI profiles that correlated significantly with his treatment response status. Our longitudinal 3D t-SNE plot analysis illustrated that the single T-lymphocytes clustered separately during the longitudinal time course of ICI and non-ICI treatment regimens, reflecting the differential treatment responses, molecular heterogeneity, and cell states of circulatory T-lymphocytes during cancer treatments.

Although our study is limited by a small cohort size, each NSCLC patient has at least two time point samples, and each sample was analyzed using novel single-cell functional proteomics profiling methods, increasing the granularity and biological depth of our analysis. Single-cell functional analysis of $CD8^+$ T-cell cytokines landscapes demonstrated the longitudinal shift of $CD8^+$ T-cell PolyFx and PSI during real-time treatment, which is not feasible in bulk cell studies. Similarly, single-cell functional analysis allows deep molecular tracking of adaptive evolutionary changes of patients' functional immune compartments under cancer immunotherapy longitudinally. Importantly, despite our small pilot cohort study size, the reported robust statistical significance and kappa coefficient of 1.0 observed in our study's ICI treatment response correlation implies a large

magnitude of clinical effects differences observed in our study cohort single cell polyfunctionality measurements. A kappa coefficient of 0.8 to 1.0 has been established to indicate a perfect agreement between the prediction and actual response status (28). Further prospective studies in larger patient cohorts are warranted to test the potential of the single T-cell ΔPolyFx and ΔPSI measures, especially combined with PD-L1 TPS, as real-time immune biomarkers in longitudinal ICI-based treatment courses to facilitate optimal treatment decision making. Since our IsoLight study platform utilizes functional single immune cells as the analytes in the longitudinal analysis, it can be more applicable to any novel immunotherapy combinations in predictive biomarkers discovery and validation, including regimens involving anti-TIGIT (43) and anti-LAG3 antibodies (44) as examples, and ICI in combination with cytotoxic chemotherapeutics. Furthermore, novel cancer therapeutics involving immune-mediated antitumor response and outcomes such as antibody-drug-conjugates (ADCs), bispecific antibodies or other emerging novel targeted/immune-mediated therapeutics could be measured and tracked using this functional real-time single-cell assay.

Our study data also nominate a potential role for peripheral $CD4^+$ T-lymphocytes ΔPSI in predicting long-term clinical survival outcomes under ICI treatments. While $CD8^+$ T-lymphocytes might be more important as determinants of early treatment response, $CD4^+$ T-cells could be more relevant and pivotal in sustaining a more durable treatment biological, cellular, and molecular response, thus translating into longer-term clinical survival outcomes (45,46). A recent report suggested that $CD4^+$ T-cell immunity in the peripheral blood correlates with ICI treatment response in NSCLC (47). The study identified that long-term ICI Rs with >500-day PFS had significantly higher numbers of $CD62L^{low}$ $CD4^+$ T-cells prior to PD-1 blockade therapy in peripheral blood, which was maintained in high percentages as a T-cell subset in long-term survivors. On the other hand, the same $CD4^+$ T-cell population was found to be decreased in those with acquired resistance after therapy. Another recent publication of a pan-cancer T-cells single-cell atlas highlighted the transcriptomic diversity of tumor-infiltrating T-cells (48). The analysis provided a sound foundation to improve our insights into the broad roles of different T-cell subtypes and cell states heterogeneity in ICI treatment response and outcomes. Of interest, Chu *et al.* [2023] identified six major subtypes of T-cells: $CD4^+$, $CD8^+$, γδ T proliferative T-cells (Tgd), natural killer T (NKT), mucosal-associated invariant T (MAIT), and proliferative T-cells (48). The $CD4^+$ T-cells represented the most abundant subset with their cellular fractions substantially varying across tissues of locations and conditions, implying their relevance in the immune dynamics of the tumor-host-therapeutics milieu under ICI treatment. There were 14 clusters of $CD8^+$ T-cells and 14 transcriptional states defined in the study. Conversely, 12 different $CD4^+$ T-cell states were defined. Interestingly, the unique stress response states in $CD8^+$ and $CD4^+$ T_{STR} cluster (stress response signature), characterized by highly expressed heat shock genes and stress response signature, were significantly upregulated in intratumoral $CD4^+$/$CD8^+$ cells following ICI treatments, especially associated with nonresponsive tumor (48). Furthermore, higher $CD4^+$ central memory T (T_{CM}) cells were found linked to increased OS in sarcoma. The $CD4^+$ T-cell memory compartment is subdivided into $CD62L^+CCR7^+$ T_{CM} cells and $CD62L^-$ $CCR7^-$ effector memory T (T_{EM}) cells (49). These cell populations are well poised in effector cytokines rapid secretion upon reactivation and engendering an enhanced secondary immune response. T_{CM} cells are functionally characterized by their IL-2 synthetic capacity and have less potential for rapid IFN-γ or IL-4 secretion. Similar to our investigation results, baseline pre-treatment specimens reported in the study by Chu *et al.* also did not achieve distinction between R and NR of single-agent ICI treatment based on the individual T-cell states, lending support to the values of longitudinal studies involving pre- and post-ICI treatment in predictive biomarkers discovery (48). Lastly, a recent preclinical study by Espinosa-Carrasco *et al.* [2024] reports that a functional triad is necessary to be established among the $CD8^+$, and $CD4^+$ T-cells along with the antigen-presenting dendritic cells in order to effectuate solid tumor cells eradication under ICI (50).

While the polyfunctionality of effector T-cells at the single cell level is shown to be an important parameter in predicting the quality of T-cell immune response and immunological control over malignant tumors, the fate of the $CD8^+$ cytotoxic T-lymphocytes and the factors that regulate the polyfunctionality of T-cells remain largely unknown. Utilizing transgenic mouse-derived $CD8^+$ T-cells that express a T-cell receptor (TCR) specific for a tumor-derived neoantigen, Imai *et al.* [2020] (51) showed that the tumor specific cytotoxic T-lymphocytes generated in the presence of $CD4^+$ T-cells displayed long persistence *in vivo* and induced enhanced tumor regression when adoptively transferred into mice with progressing tumor. Our study data on the role of $CD4^+$ ΔPSI predicting a strong trend of

PFS and OS in ICI-treated NSCLC patients add further support to the notion of $CD4^+$ T-cells positively impacting the polyfunctionality of cytotoxic $CD8^+$ T-cells in their survival and memory formation associated with tumoral immunological control and subsequent long-term clinical survival outcomes (51). Lastly, peripheral circulating $CD4^+$ T-cell immunity such as activated $CD4^+$ T_{EM} clonal expansion, may have a role in the emergence of irAEs from ICI blockade as well (52). Importantly, a number of literature reports in recent years provided strong support correlating irAEs and ICI treatment response as well as OS outcomes in human cancers, including NSCLC (53-55).

There are several limitations in our current study. First, this study represents a proof-of-concept study with a relatively small study cohort size. However, we do have inclusion of both healthy subject donors as well as NSCLC disease subjects for comparison. Given the single cell levels of molecular cytokine analysis of each patient blood sample and the dynamic evaluation of pre- and post-treatment samples in our study, the limitations of small study cohort were partially mitigated. Furthermore, the statistical significance demonstrated in our results in the $CD8^+$ T-cells ΔPolyFx and ΔPSI discriminating ICI treatment Rs *vs.* NRs, better than PD-L1 TPS alone, highlights the likely strong magnitude of treatment effects differences discerned through single cell analysis even in a small cohort of study subjects. Second, the need for pre- and post-treatment samples under ICI therapy regimens as the basis of predictive biomarkers would exclude characterizing pretreatment baseline samples for ICI treatment patient selection. However, this is already the current clinical paradigm in the use of ICI especially in the setting of combination chemoimmunotherapy both in advanced stage and in resectable stage neoadjuvant use where PD-L1 TPS is not prerequisite of the therapies and does not help in patient selection (34-36). Moreover, measuring dynamically and longitudinally peripheral single T-cells as ICI biomarkers would relieve the need for repeated tumoral biopsies to assess tumoral PD-L1 expression to monitor patients' treatment course and response-resistance profile and evolution. Third, our study does not specifically establish the differential predictive biomarker capabilities among different ICI treatment regimens, namely PD-1/PD-L1 single agent treatment versus chemoimmunotherapy, and does not differentiate among different chemotherapeutic regimens in combination with the ICI. Lastly, the current cost of instrumentation, materials and reagents for the IsoLight single T-cell polyfunctionality assays is considerably high, limiting the scalability and clinical applicability at the present time. Nonetheless, this is invariably true for most if not all of emergent novel technologies, as evidenced in the recent history of the development of genome sequencing and single cell genomics-transcriptomics platforms. Just as there was rapid decline in the cost per genome sequencing throughout the journey of human genome sequencing over the past decade, novel single cell proteomics platforms and methodologies would most likely see a rapid decline in the underlying cost with time.

Conclusions

In summary, our proof-of-concept study in longitudinal live single-cell cytokine profiling analysis of peripheral blood immune T-lymphocytes nominated single $CD8^+$ T-cells polyfunctionality measurements as a promising potential predictive biomarker for PD-1/PD-L1 ICI treatment in NSCLC for tumor response, whereas single $CD4^+$ T-cells polyfunctionality measurements may have relevance in longer-term ICI treatment survival outcomes correlation. Our study findings warrant further investigations in larger study cohorts and prospective ICI treatment trials to shed more confirmatory light on the utility of the novel real-time liquid biopsies with T-lymphocytes ΔPSI to determine immunotherapy predictive biomarker for optimized clinical applications for NSCLC ICI-based therapies.

Acknowledgments

We thank the Dr. Frank and Franco Cancer Research Endowment, GLY Foundation Cancer Research Endowment, Vernon M. and Jolene E. Chinchilli Family Endowment for Cancer Research, and also the Highmark Community Health Reinvestment Fund of the Penn State Cancer Institute, Penn State College of Medicine, Penn State University, for the support of P.C.M.
Funding: None.

Footnote

Reporting Checklist: The authors have completed the REMARK reporting checklist. Available at https://tlcr.amegroups.com/article/view/10.21037/tlcr-24-260/rc

Data Sharing Statement: Available at https://tlcr.amegroups.com/article/view/10.21037/tlcr-24-260/dss

Peer Review File: Available at https://tlcr.amegroups.com/

article/view/10.21037/tlcr-24-260/prf

Conflicts of Interest: All authors have completed the ICMJE uniform disclosure form (available at https://tlcr.amegroups.com/article/view/10.21037/tlcr-24-260/coif). P.C.M. received consulting honorarium from AstraZeneca, BeiGene, Pfizer and Daiichi Sankyo; and conference traveling support from DAVA Oncology; and clinical trial research grants to the institution from Apollomics, BeiGene, AstraZeneca, OncoC4, GenMab, Elevation Oncology, Merck, AbbVie and Mirati. The other authors have no conflicts of interest to declare.

Ethical Statement: The authors are accountable for all aspects of the work in ensuring that questions related to the accuracy or integrity of any part of the work are appropriately investigated and resolved. The study was conducted in accordance with the Declaration of Helsinki (as revised in 2013). The study was approved by the Institutional Review Board of West Virginia University (WVU011117, 2016), and by the Institutional Review Board of Penn State Milton S. Hershey Medical Center (STUDY00005272, 2016) and informed consent was obtained from all individual participants.

References

1. American Cancer Society. Cancer Facts & Figures 2024. Atlanta: American Cancer Society; 2024.
2. Korman AJ, Garrett-Thomson SC, Lonberg N. The foundations of immune checkpoint blockade and the ipilimumab approval decennial. Nat Rev Drug Discov 2022;21:509-28.
3. Marrone KA, Brahmer JR. Immune Checkpoint Therapy in Non-Small Cell Lung Cancer. Cancer J 2016;22:81-91.
4. Sun Q, Hong Z, Zhang C, et al. Immune checkpoint therapy for solid tumours: clinical dilemmas and future trends. Signal Transduct Target Ther 2023;8:320.
5. Mountzios G, Remon J, Hendriks LEL, et al. Immune-checkpoint inhibition for resectable non-small-cell lung cancer - opportunities and challenges. Nat Rev Clin Oncol 2023;20:664-77.
6. Holder AM, Dedeilia A, Sierra-Davidson K, et al. Defining clinically useful biomarkers of immune checkpoint inhibitors in solid tumours. Nat Rev Cancer 2024;24:498-512.
7. Bodor JN, Boumber Y, Borghaei H. Biomarkers for immune checkpoint inhibition in non-small cell lung cancer (NSCLC). Cancer 2020;126:260-70.
8. Won SE, Park HJ, Byun S, et al. Impact of pseudoprogression and treatment beyond progression on outcome in patients with non-small cell lung cancer treated with immune checkpoint inhibitors. Oncoimmunology 2020;9:1776058.
9. Mazieres J, Drilon A, Lusque A, et al. Immune checkpoint inhibitors for patients with advanced lung cancer and oncogenic driver alterations: results from the IMMUNOTARGET registry. Ann Oncol 2019;30:1321-8.
10. Akbay EA, Koyama S, Carretero J, et al. Activation of the PD-1 pathway contributes to immune escape in EGFR-driven lung tumors. Cancer Discov 2013;3:1355-63.
11. Arcila ME, Oxnard GR, Nafa K, et al. Rebiopsy of lung cancer patients with acquired resistance to EGFR inhibitors and enhanced detection of the T790M mutation using a locked nucleic acid-based assay. Clin Cancer Res 2011;17:1169-80.
12. Benedettini E, Sholl LM, Peyton M, et al. Met activation in non-small cell lung cancer is associated with de novo resistance to EGFR inhibitors and the development of brain metastasis. Am J Pathol 2010;177:415-23.
13. Calles A, Riess JW, Brahmer JR. Checkpoint Blockade in Lung Cancer With Driver Mutation: Choose the Road Wisely. Am Soc Clin Oncol Educ Book 2020;40:372-84.
14. Socinski MA, Jotte RM, Cappuzzo F, et al. Atezolizumab for First-Line Treatment of Metastatic Nonsquamous NSCLC. N Engl J Med 2018;378:2288-301.
15. Schoenfeld AJ, Rizvi H, Bandlamudi C, et al. Clinical and molecular correlates of PD-L1 expression in patients with lung adenocarcinomas. Ann Oncol 2020;31:599-608.
16. Samstein RM, Lee CH, Shoushtari AN, et al. Tumor mutational load predicts survival after immunotherapy across multiple cancer types. Nat Genet 2019;51:202-6.
17. Veldore VH, Choughule A, Routhu T, et al. Validation of liquid biopsy: plasma cell-free DNA testing in clinical management of advanced non-small cell lung cancer. Lung Cancer (Auckl) 2018;9:1-11.

18. Liu S, Wang J. Current and Future Perspectives of Cell-Free DNA in Liquid Biopsy. Curr Issues Mol Biol 2022;44:2695-709.
19. van der Leun AM, Thommen DS, Schumacher TN. CD8(+) T cell states in human cancer: insights from single-cell analysis. Nat Rev Cancer 2020;20:218-32.
20. Osorio JC, Arbour KC, Le DT, et al. Lesion-Level Response Dynamics to Programmed Cell Death Protein (PD-1) Blockade. J Clin Oncol 2019;37:3546-55.
21. Liu H, Zhang T, Ye J, et al. Tumor-infiltrating lymphocytes predict response to chemotherapy in patients with advance non-small cell lung cancer. Cancer Immunol Immunother 2012;61:1849-56.
22. Heath JR, Ribas A, Mischel PS. Single-cell analysis tools for drug discovery and development. Nat Rev Drug Discov 2016;15:204-16.
23. Chattopadhyay PK, Gierahn TM, Roederer M, et al. Single-cell technologies for monitoring immune systems. Nat Immunol 2014;15:128-35.
24. Stubbington MJT, Rozenblatt-Rosen O, Regev A, et al. Single-cell transcriptomics to explore the immune system in health and disease. Science 2017;358:58-63.
25. Baysoy A, Bai Z, Satija R, et al. The technological landscape and applications of single-cell multi-omics. Nat Rev Mol Cell Biol 2023;24:695-713.
26. Ginhoux F, Yalin A, Dutertre CA, et al. Single-cell immunology: Past, present, and future. Immunity 2022;55:393-404.
27. Xue Q, Bettini E, Paczkowski P, et al. Single-cell multiplexed cytokine profiling of CD19 CAR-T cells reveals a diverse landscape of polyfunctional antigen-specific response. J Immunother Cancer 2017;5:85.
28. Landis JR, Koch GG. The measurement of observer agreement for categorical data. Biometrics 1977;33:159-74.
29. Duchemann B, Friboulet L, Besse B. Therapeutic management of ALK+ nonsmall cell lung cancer patients. Eur Respir J 2015;46:230-42.
30. Parvaresh H, Roozitalab G, Golandam F, et al. Unraveling the Potential of ALK-Targeted Therapies in Non-Small Cell Lung Cancer: Comprehensive Insights and Future Directions. Biomedicines 2024;12:297.
31. Robert C. A decade of immune-checkpoint inhibitors in cancer therapy. Nat Commun 2020;11:3801.
32. Kibirova A, Mattes MD, Smolkin M, et al. The Journey of an EGFR-Mutant Lung Adenocarcinoma through Erlotinib, Osimertinib and ABCP Immunotherapy Regimens: Sensitivity and Resistance. Case Rep Oncol 2019;12:765-76.
33. Felip E, Altorki N, Zhou C, et al. Adjuvant atezolizumab after adjuvant chemotherapy in resected stage IB-IIIA non-small-cell lung cancer (IMpower010): a randomised, multicentre, open-label, phase 3 trial. Lancet 2021;398:1344-57.
34. Forde PM, Spicer J, Lu S, et al. Neoadjuvant Nivolumab plus Chemotherapy in Resectable Lung Cancer. N Engl J Med 2022;386:1973-85.
35. Wakelee H, Liberman M, Kato T, et al. Perioperative Pembrolizumab for Early-Stage Non-Small-Cell Lung Cancer. N Engl J Med 2023;389:491-503.
36. Lu S, Zhang W, Wu L, et al. Perioperative Toripalimab Plus Chemotherapy for Patients With Resectable Non-Small Cell Lung Cancer: The Neotorch Randomized Clinical Trial. JAMA 2024;331:201-11.
37. Olivares-Hernández A, González Del Portillo E, Tamayo-Velasco Á, et al. Immune checkpoint inhibitors in non-small cell lung cancer: from current perspectives to future treatments-a systematic review. Ann Transl Med 2023;11:354.
38. Anagnostou V, Landon BV, Medina JE, et al. Translating the evolving molecular landscape of tumors to biomarkers of response for cancer immunotherapy. Sci Transl Med 2022;14:eabo3958.
39. Anagnostou V, Ho C, Nicholas G, et al. ctDNA response after pembrolizumab in non-small cell lung cancer: phase 2 adaptive trial results. Nat Med 2023;29:2559-69.
40. Oloomi M, Moazzezy N, Bouzari S. Comparing blood versus tissue-based biomarkers expression in breast cancer patients. Heliyon 2020;6:e03728.
41. Mamdani H, Ahmed S, Armstrong S, et al. Blood-based tumor biomarkers in lung cancer for detection and treatment. Transl Lung Cancer Res 2017;6:648-60.
42. Bian S, Hou Y, Zhou X, et al. Single-cell multiomics sequencing and analyses of human colorectal cancer. Science 2018;362:1060-3.
43. Rovers S, Janssens A, Raskin J, et al. Recent Advances of Immune Checkpoint Inhibition and Potential for (Combined) TIGIT Blockade as a New Strategy for Malignant Pleural Mesothelioma. Biomedicines 2022;10:673.
44. Anderson AC, Joller N, Kuchroo VK. Lag-3, Tim-3, and TIGIT: Co-inhibitory Receptors with Specialized Functions in Immune Regulation. Immunity 2016;44:989-1004.
45. Oh DY, Kwek SS, Raju SS, et al. Intratumoral CD4(+) T Cells Mediate Anti-tumor Cytotoxicity in Human Bladder Cancer. Cell 2020;181:1612-1625.e13.

46. González-Navajas JM, Elkord E, Lee J. Editorial: CD4+ T Cells in Cancer Immunotherapies. Front Immunol 2021;12:737615.
47. Kagamu H, Kitano S, Yamaguchi O, et al. CD4(+) T-cell Immunity in the Peripheral Blood Correlates with Response to Anti-PD-1 Therapy. Cancer Immunol Res 2020;8:334-44.
48. Chu Y, Dai E, Li Y, et al. Pan-cancer T cell atlas links a cellular stress response state to immunotherapy resistance. Nat Med 2023;29:1550-62.
49. Sallusto F, Lenig D, Förster R, et al. Two subsets of memory T lymphocytes with distinct homing potentials and effector functions. Nature 1999;401:708-12.
50. Espinosa-Carrasco G, Chiu E, Scrivo A, et al. Intratumoral immune triads are required for immunotherapy-mediated elimination of solid tumors. Cancer Cell 2024;42:1202-1216.e8.
51. Imai N, Tawara I, Yamane M, et al. CD4(+) T cells support polyfunctionality of cytotoxic CD8(+) T cells with memory potential in immunological control of tumor. Cancer Sci 2020;111:1958-68.
52. Earland N, Zhang W, Usmani A, et al. CD4 T cells and toxicity from immune checkpoint blockade. Immunol Rev 2023;318:96-109.
53. Abu-Sbeih H, Tang T, Ali FS, et al. The Impact of Immune Checkpoint Inhibitor-Related Adverse Events and Their Immunosuppressive Treatment on Patients' Outcomes. J Immunother Precis Oncol 2020;1:7-18.
54. Owen DH, Wei L, Bertino EM, et al. Incidence, Risk Factors, and Effect on Survival of Immune-related Adverse Events in Patients With Non-Small-cell Lung Cancer. Clin Lung Cancer 2018;19:e893-900.
55. Albandar HJ, Fuqua J, Albandar JM, et al. Immune-Related Adverse Events (irAE) in Cancer Immune Checkpoint Inhibitors (ICI) and Survival Outcomes Correlation: To Rechallenge or Not? Cancers (Basel) 2021;13:989.

Cite this article as: Lim ZF, Wu X, Zhu L, Albandar H, Hafez M, Zhao C, Almubarak M, Smolkin M, Zheng H, Wen S, Ma PC. Quantitative peripheral live single T-cell dynamic polyfunctionality profiling predicts lung cancer checkpoint immunotherapy treatment response and clinical outcomes. Transl Lung Cancer Res 2024;13(12):3323-3343. doi: 10.21037/tlcr-24-260

